

Full Length Research Paper

First-principles study on electronic and optical properties of La-doped ZnS

Hai-Qing Xie¹, Yun Zeng^{1*}, Wei-Qing Huang¹, Li Peng², Ping Peng² and Tai-Hong Wang¹

¹School of Physics and Microelectronics Science, Hunan University, Changsha 410082, Peoples Republic of China.

²College of Material and Engineering, Hunan University, Changsha 410082, Peoples Republic of China.

Accepted 26 November, 2010

Using the first principle plane-wave pseudo potential method, a systematic investigation on electronic and optical properties of ZnS with and without La-doping has been performed. Calculation results show that La-doping narrows the band gap of ZnS systems and La doped ZnS system changes from semiconductor into metal through the Mott transition. Moreover, with La-doping increasing, the decrease of absorption coefficient and redshift of absorption spectra are obtained. Absorption spectra of pure ZnS and La-doped ZnS are in good agreement with the experimental results.

Key words: La-doped ZnS, optical properties, electronic properties, first-principles calculations.

INTRODUCTION

Zinc sulfide is an important semiconductor compound of the II to VI group with wide band-gap of 3.68 eV (corresponding to wavelength of 337 nm) at 300°K (Bredal and Merikhi, 1998). Consequently, it is a potentially important material to be used as windows layers for solar cells (Bloss et al., 1988). It is an important device material for the detection, emission and modulation of visible and near ultraviolet light (Saravanan et al., 2010; Marquerdt et al., 1994).

Moreover, ZnS is believed to be one of the most promising materials for blue-light diodes (Hasse et al., 1991) and electro-luminescent displays (Göde et al., 2007; Roy et al., 2006).

During the past decade, ZnS based luminescence materials have been studied extensively. Particularly, ZnS nanocrystallites doped with an optically active luminescence center create new opportunities for luminescent study and application of nanometer scale material (Ping et al., 2002). Doped with transition-metal element or rare-earth element, ZnS can be used as effective phosphor materials (Yamaguchi et al., 1999). Gallagher et al. (1994) investigated the optical properties

of Mn-doped nanocrystals of ZnS. The external photoluminescent quantum efficiency of Mn-doped nanocrystals ZnS is up to 18% and increases with decreasing size of the particles (Gallagher et al., 1994). Comparing to pure ZnS nanocrystals, Eu³⁺-doped ZnS nanocrystals have high luminescence efficiency, and the peak of higher energy is slightly blue shifted with an increase of the doping level (Qu et al., 2002). The preparation of Fe and Ni doped ZnS nanocrystals by using mercaptoethanol to passivate the surface of the particles are also reported. The optical absorption spectra of ZnS nanocrystals show a blue shift in the absorption edge with increasing Fe-content (Sambasivam et al., 2009; Soni et al., 2009; Huang et al., 2009).

Co²⁺ doped ZnS samples enhance visible light emission with emission intensities of 35 times larger than that of the undoped samples (Sarkar et al., 2009). Studies on La-doped ZnS thin films/nanocrystals have, however, not been reported so far.

In this paper, we study the electronic and optical properties of ZnS with and without La-doping using “first-principles calculations” based density functional theory (DFT) in “material studio” 4.0. Our results show that the existence of doped La atom leads to narrower energy gap and the Mott transition (that is, from semiconductor into metal) of La-doped ZnS. Moreover, the absorption threshold of La-doped ZnS systems is considerably

*Corresponding author. E-mail: zengyun@hnu.cn. Tel/Fax: +86-731-88822332.

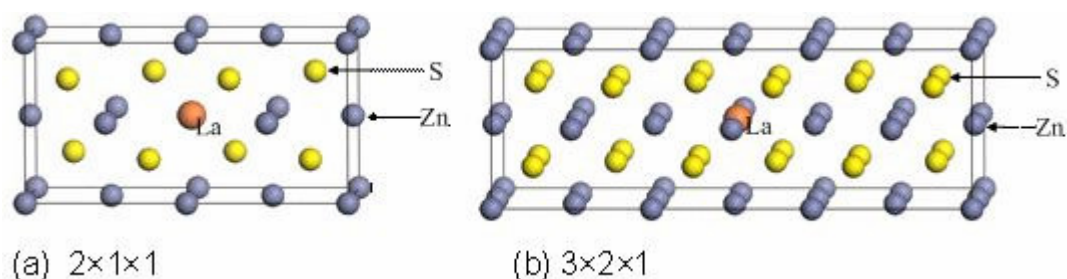


Figure 1. ZnS supercells for calculation.

Table 1. Models of ZnS Supercell.

Models	Atoms number	Concentration of doped La (at %)
M-1 Zn_8S_8	16 (Zn: 8, S: 8)	—
M-2 $Zn_7(La)S_8$	16 (Zn: 7, S: 8, La: 1)	12.5
M-3 $Zn_{23}(La)S_{24}$	48 (Zn: 23, S: 24, La: 1)	4.17

redshifted. These results are verified by the experiment.

METHODS OF CALCULATION AND EXPERIMENT

Sphalerite ZnS was adopted in the calculation. A series of ZnS supercell with and without La-doping were constructed and calculated to investigate the effect of La on the properties of ZnS, as depicted in Figure 1 and Table 1. The doped La atom occupied the central Zn atom in the supercell models.

Numerical calculations were carried out by CASTEP in material studio 4.0 based on first principles (Payne et al., 1992; Segall et al., 2002). Ultrasoft pseudo potential was used to describe the electron-ion interaction (Vanderbilt, 1990). The energy cutoff (E_{cut}) of plane wave functions was set at 350.0 eV. All atomic positions in the ZnS supercell have been relaxed according to the total energy and force using the BFGS scheme, based on the cell optimization criterion (RMS force of 0.01 eV/Å, stress of 0.02 GPa, and displacement of 5.0×10^{-4} Å) (Fischer and Almóf, 1992). The calculation of total energy and electronic is followed by cell optimization with SCF tolerance of 5.0×10^{-6} eV/atom under GGA-PBE potential (Perdew et al., 1996).

In order to verify the calculation results, undoped and La-doped ZnS thin films were prepared by chemical bath deposition (CBD) process on conductive glasses through the coprecipitation reaction of inorganic precursors zinc sulfate, thiosulfate ammonia and La_2O_3 . The detailed experimental procedure will be given elsewhere.

RESULTS AND DISCUSSION

Structural optimization

To assess the accuracy of our computation method, we performed a series of calculations for cell optimization. The equilibrium lattice constant after optimization is $a=b=c=0.54194$ nm, which is good agreement with the

experimental results ($a=b=c=0.54093$ nm) (Gallagher et al., 1994). Thus, the same calculation condition was adopted to calculate the geometrical, electronic and energetic structures of the ZnS with and without La-doping.

Electronic structure

Figure 2 illustrates the energy band structure, partial and total electronic density of states (PDOS and DOS) of pure ZnS supercell system showed in Figure 1. Zero of the band structure in Figure 2 is Fermi energy level. The bottom of conduction band and top of valence band both locate at G point, which is the representative characteristic for direct transition semiconductor. In local density functional theory, neglecting of excitation state during Kohn-Sham function's calculation results in lower energy levels above valence band in calculation energy band than that of experimental results. While, the energy levels below valence band in calculation are consistent with the experimental results. Thus, the energy gap in first principle calculation based on local density functional theory is about 30 to 50% lower than experimental values. In our calculation, the energy gap of pure ZnS, E_g , is equal to 2.18 eV which is obviously lower than experimental results ($E_g=3.68$ eV). Subsequently, scissors correction with value of 1.50 eV was adopted.

As shown in Figure 2, conduction band mainly dominated by the valence electrons of Zn (4s) and S (3p) orbits in the pure ZnS system mainly locates in the 4.0 to 8.8 eV energy range. A significant charge transfer from Zn (4s) to S (3p) orbits shown in Table 2 and a overlap

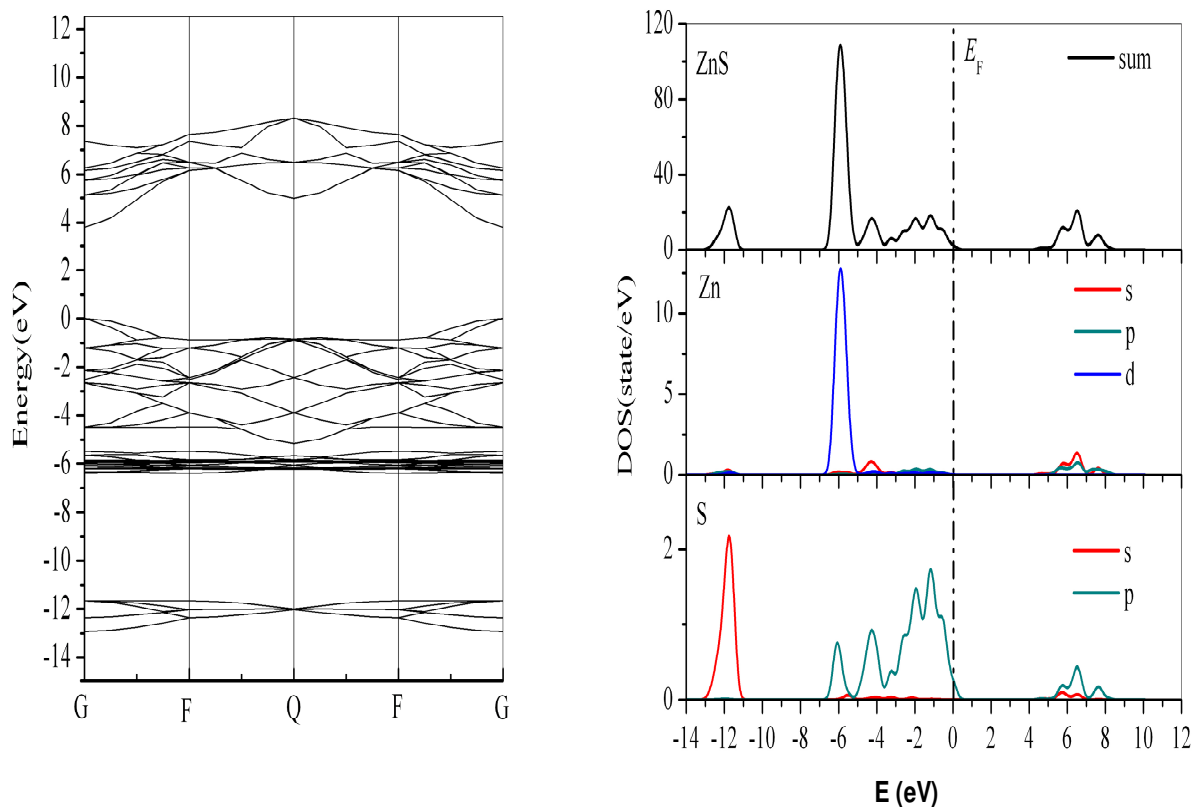


Figure 2. Energy band structure and DOS of pure ZnS supercell.

Table 2. Mulliken charge $Q(A)$ of the atoms in the ZnS supercells.

Models	$Q(\text{Zn})$	$Q(\text{S})$	$Q(\text{La})$
M-1	0.48	-0.48	—
M-2	0.03	-0.51	1.81
M-3	0.35	-0.52	1.40

between the Zn (4s) and S (3p) valence electrons depicted in Figure 2 reveals strong ionic bonding and weak covalent bonding between the FNN (first nearest neighbor) Zn-S in pure ZnS. Valence band in pure is mainly combined by two part, that, top valence band (-5.2 to 0 eV) and bottom valence band (-6.8 to -5.1 eV), as illustrated in Figure 2. It is worth noting that the top valence band and bottom valence band are mainly contributed by S (3p) and Zn (3d) orbits, respectively. In addition, the Zn (4s)-S (3p) hybridization at -4.0 eV between the FNN Zn-S is observed.

The energy band structures and DOS in $2 \times 1 \times 1$ (M-2) and $3 \times 2 \times 1$ (M-3) ZnS supercell with La-doping are respectively depicted in Figures 3 and 4. Compared to the pure ZnS supercell model, the doped La atoms lead to a notable variation of the energy band structure in the

La doped ZnS systems. For La doped ZnS systems, the bottom of conduction band and the top of valence band both move toward the lower energy level. However, variation extent of the former is much larger than the latter one. Therefore, energy gap in ZnS system with La-doping deduces comparing to the pure ZnS system, such as 1.89 eV and 2.10 eV for the M-2 and M-3 models, respectively, as shown in Figures 3 and 4.

Total DOS is separated to three regions in higher concentration La-doping ZnS system (M-2), that is, higher energy region ((-1) to 3 eV), lower energy region ((-2.9) to (-9.2) eV) and the energy region below -14eV, as given in Figure 3. For the higher energy region, the bonding electrons mainly come from the valence electrons of La (d) orbits. The bonding electrons in the lower energy region are mainly contributed by the valence electron of

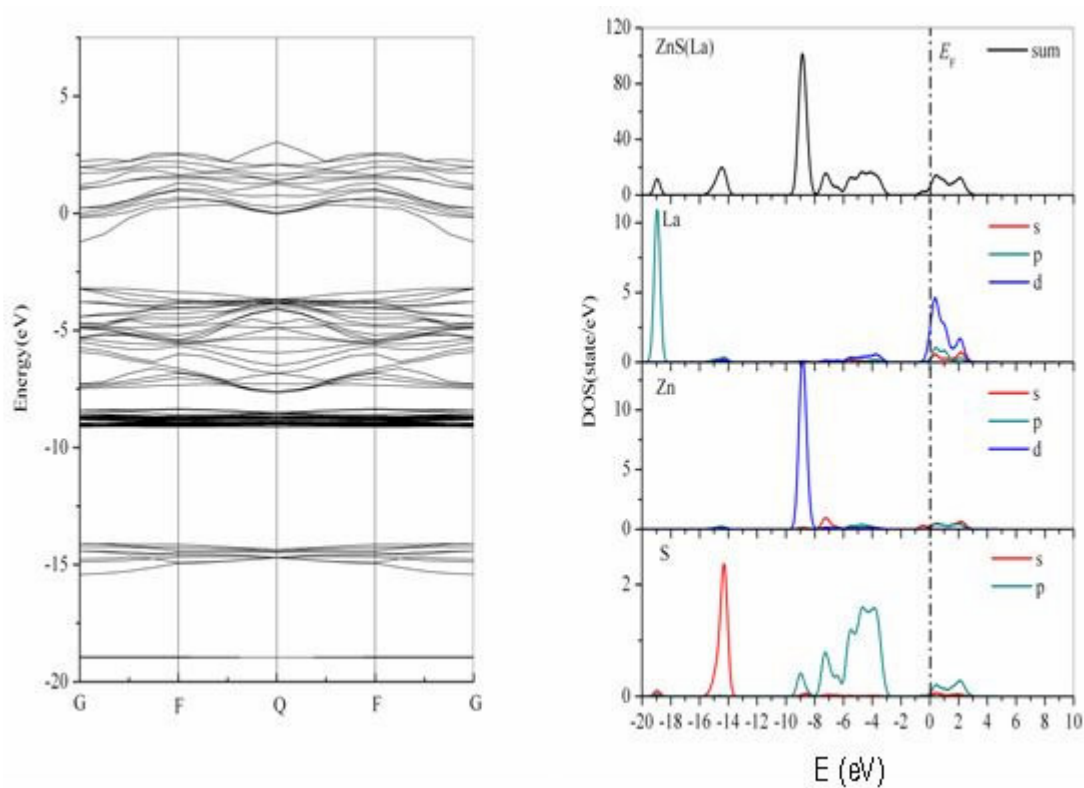


Figure 3. Energy band structure and DOS of $2 \times 1 \times 1$ (M-2) ZnS supercell with La-doping.

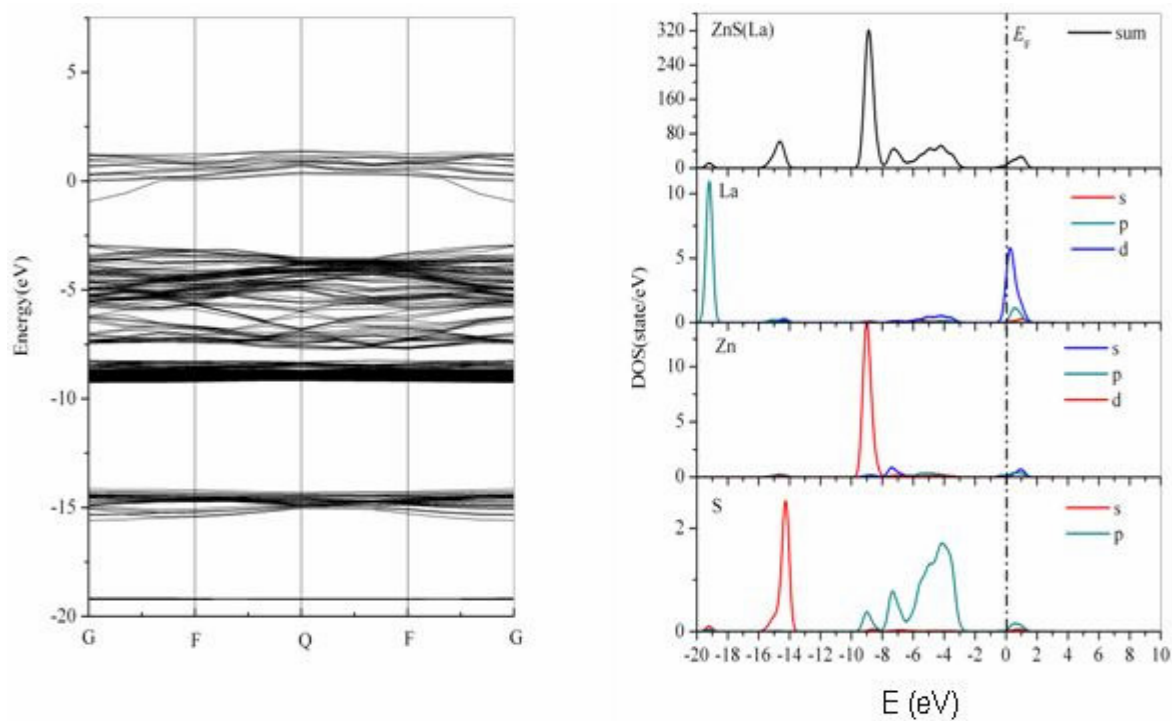


Figure 4. Energy band structure and DOS of $3 \times 2 \times 1$ (M-3) ZnS supercell with La-doping.

Zn (d) and S (p) orbitals. While, the bonding electrons below -14 eV mainly originate from the contribution of valence electron of S (s) and La (p) orbitals.

As discussed above, due to the bonding electrons in higher energy region mainly came from the valence electrons of La (d) orbitals. In addition, only weak metallic bonding between the FNN La-Zn is observed in La doped ZnS systems. Thus, fewer bonding electrons near the Fermi energy level in lower concentration La doped ZnS supercell (M-3) are achieved comparing with M-2, as shown in Figure 4.

As obviously shown in the Figures 3 and 4, the main peak of the doped La atoms, which is mainly contributed by the La (5d) valence charge, locate near the Fermi energy level, indicating that the metallic bonding between the doped La atom and its FNN atoms in La-doped ZnS supercell models. As given in Table 2, one La atom losses 1.81 electrons and 1.40 electrons, and its FNN one Zn atom losses 0.03 electrons and 0.35 electrons, while, one S atom nearby La atom accepts 0.51 electrons and 0.52 electrons, respectively, in La-doped ZnS supercell models M2 and M3. These results mean that more than one free electron exists in La-doped ZnS supercells, and it may results in metallization of the La-doped ZnS systems.

In order to further investigate the influence induced by La-doping on electronic interaction, the charge density contour plots on the (001) and (110) plane of the ZnS supercell with and without La-doping are presented in Figures 5 and 6. As obviously shown in Figure 5, for the pure ZnS supercell model, the electronic interaction between central Zn atom and its neighboring atoms is obviously isotropic. On the contrary, after La-doping, the La atom with larger atomic radius may push its FNN host atoms away and further affects the electronic distribution in the supercell. As a consequence, significant anisotropic build-up of the directional bonding charge of La atom can be observed. In addition, from Figure 6, the repellency between S and La results in the increasing of La-S distance and decreasing of S-Zn distance. However, no discernible difference of electronic distribution around the host atoms, which are farther from doped La atom, in La-doped ZnS models and in pure ZnS models, could be easily recognized.

Optical properties

Absorption spectra of the undoped ZnS and La-doped ZnS with different concentrations of lanthanum ions are shown in Figure 7. From Figure 7, the absorption threshold of pure ZnS is about 3.6 eV, corresponding to band gap of 3.68 eV. The peak value of absorption spectrum in pure ZnS located at 8.5 eV, which is the results of charge transfer from the S-3p (-1.5 eV) to the Zn-4s (6.5 eV) orbitals. However, certain difference exists

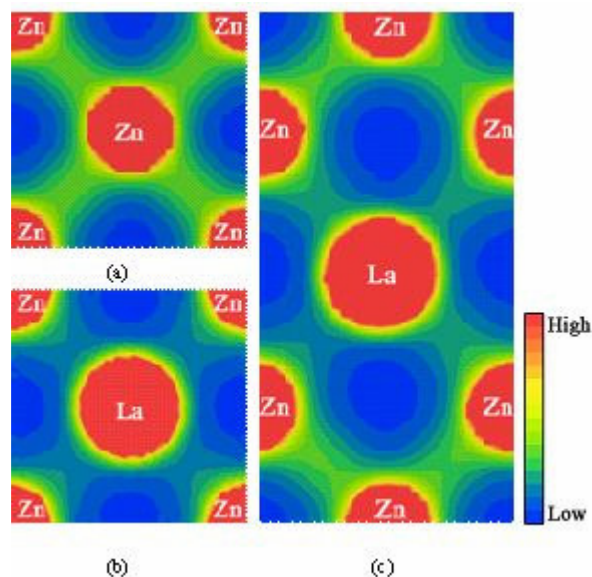


Figure 5. Charge density contour plots on the (001) plane of the ZnS supercell with and without La-doping. (a) M-1 (b) M-2 (c) M-3.

between peak value's location and charge transfer energy due to relaxation effects in electron transfer process. Compared to pure ZnS, considerable redshift of absorption threshold in La-doped ZnS systems are achieved due to narrower energy gap in ZnS systems with La doping, as depicted in Figures 3 and 4. In addition, the peak value of absorption coefficient decreases with the increasing La content in La-doped ZnS models.

The absorption spectra of the ZnS thin films prepared by CBD are displayed in Figure 8. It can be seen from Figure 8 that the absorptivity of the La-doped ZnS thin films is smaller than that of undoped ZnS thin films. Moreover, the higher the La-doped concentration, the lower the absorptivity. Also, a considerable red shift in the absorption spectra is achieved with the increasing La content in La-doped ZnS thin films. These results are consistent with the calculation results, as shown in Figure 7.

Conclusions

Using a first principles plane wave pseudopotential method, the electronic structures and optical properties of La-doped ZnS system have been investigated. A series of ZnS supercell models were constructed and the energy band structures, (DOS) and (PDOS) of ZnS systems were calculated and analyzed. Results show that, obvious variation and narrower energy gap of energy band structures are achieved in ZnS system with La-

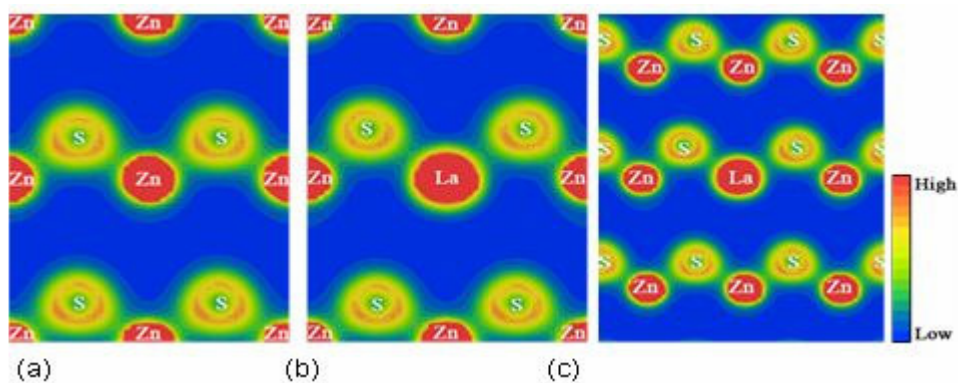


Figure 6. Charge density contour plots on the (110) plane of the ZnS supercell with and without La-doping. (a) M-1 (b) M-2 (c) M-3.

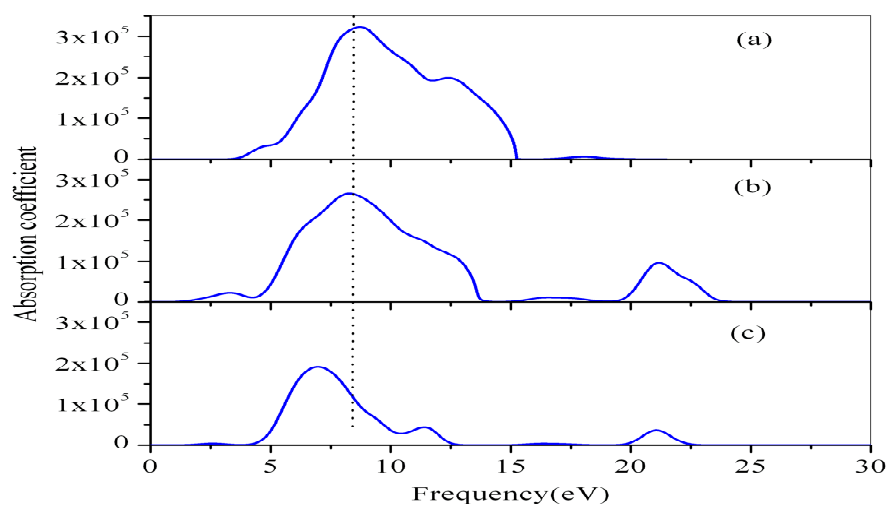


Figure 7. Calculation results of absorption spectra in the ZnS supercell. (a) without La-doping (b) and (c) for M-3 and M-2, respectively.

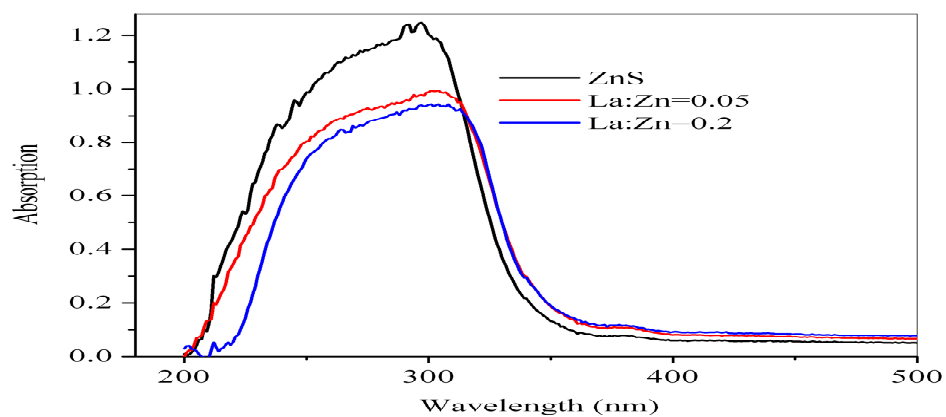


Figure 8. Measurement results of absorption spectra in the ZnS thin films with and without La-doping.

doping. The DOS peak of the doped La atoms mainly contributed by the La 5d valence charge locates near the Fermi energy level, which results in the metallization of the La doped ZnS systems. Significant anisotropic build-up of the directional bonding charge of La atom could be observed. In addition, optical characteristics of ZnS systems were studied. Decreasing of absorption coefficient and redshift of absorption threshold are obtained with increasing La doping concentration in ZnS systems, which are well consistent with measurement results of pure ZnS and La doped ZnS thin films.

ACKNOWLEDGMENTS

This work was contained in the project 61040061 supported by National Natural Science Foundation of China. It is also supported by Hunan Provincial Innovation Foundation for Postgraduate.

REFERENCES

- Bloss WH, Pfisterer F, Schock HW (1988). Advances in solar energy, an annual review of research and development, in: K.W. Boer, J.A. Duffie (Eds.), American Solar Energy Society Inc., New York, 4: 275.
- Bredal M, Merikhi J (1998). ZnS precipitation: morphology control. *J. Mat. Sci.*, 33: 471-476.
- Fischer TH, Almöf J (1992). General Methods for Geometry and Wave Function Optimization. *J. Phys. Chem.*, 96: 9768-9774.
- Gallagher D, Hong X, Nurmikko A (1994). Optical properties of manganese-doped nanocrystals of ZnS. *Physical Rev. Lett.*, 72: 416-419.
- Göde F, Gümüs C, Zor M (2007). Investigations on the physical properties of the polycrystalline ZnS thin films deposited by the chemical bath deposition method. *J. Crystal Growth*, 299: 136-141.
- Hasse MA, Qiu J, DePuydt JM, Cheng H (1991). Blue-green laser diode. *Appl. Phys. Lett.*, 59: 1272-1274.
- Huang CM, Chen LC, Pan GT, Yang CK, Chang WS, Cheng KW (2009). Effect of Ni on the growth and photoelectrochemical properties of ZnS thin films. *Materials Chem. Phys.*, 117: 156-162.
- Marquardt E, Optiz B, Scholl M, Henker M (1994). Electro absorption and light modulation with ZnSe/ZnSSe multi-quantum wells grown by metalorganic vapor phase epitaxy. *J. Appl. Phys.*, 75: 8022-8025.
- Payne MC, Teter MP, Allan DC, Arias TA, Joannopoulos JD (1992). Iterative minimization techniques for ab initio total-energy calculations molecular dynamics and conjugate gradients. *Rev. Modern Phys.*, 64: 1045-1097.
- Perdew JP, Burke K, Ernzerhof M (1996). Generalized Gradient Approximation Made Simple. *Phys. Rev. Lett.*, 77: 3865-3868.
- Ping Y, Chunfeng S, Mengkai L, Guangjun Z, Zhongxi Y, Dong X, Duorong Y (2002). Photoluminescence of Cu⁺-doped and Cu²⁺-doped ZnS nanocrystallites. *J. Phys. Chem. Solids.*, 63: 639-643.
- Qu S, Zhou WH, Liu FQ, Chen NF, Wang ZG, Pan HY, Yu DP (2002). Photoluminescence properties of Eu-doped ZnS nanocrystals prepared in a water/methanol solution. *Appl. Phys. Lett.*, 80: 3605-3607.
- Roy P, Ota JR, Srivastava SK (2006). Crystalline ZnS thin films by chemical bath deposition method and its characterization. *Thin Solid Films*, 515: 1912-1917.
- Sambasivam S, Reddy BK, Divya A, Madhusudhana Rao N, Jayasankar CK, Sreedhar B (2009). Optical and ESR studies on Fe doped ZnS nanocrystals. *Phys. Lett. A.*, 373: 1465-1468.
- Saravanan R, Saravanakumar S, Lavanya S (2010). Growth and local structure analysis of ZnS nano particles. *Physica B.*, 405: 3700-3703.
- Sarkar R, Tiwary CS, Kumbhakar P, Mitra AK (2009). Enhanced visible light emission from Co²⁺ doped ZnS nanoparticles. *Physica B.*, 404: 3855-3858.
- Segall MD, Lindan PJD, Probert MJ, Pickard CJ, Hasnip PJ, Clark SJ, Payne MC (2002). First-principles simulation: ideas, illustrations and the CASTEP code. *J. Phys. Condens. Matter.* 14: 2717-2744.
- Soni H, Chawda M, Bodas D (2009). Electrical and optical characteristics of Ni doped ZnS clusters. *Materials Lett.*, 63: 767-769.
- Vanderbilt D (1990). Soft self-consistent pseudopotentials in a generalized eigenvalue formalism. *Phys. Rev. B.*, 41: 7892-7895.
- Yamaguchi T, Yamamoto Y, Tanaka T, Yoshida A (1999). Preparation and characterization of (Cd,Zn)S thin films by chemical bath deposition for photovoltaic devices. *Thin Solid Films*, 343-344: 516-519.